Heterogeneous & Homogeneous & Bio- & Nano-

CHEMCATCHEM

CATALYSIS

Title: Efficient Conversion of Bio-lactic Acid to 2,3-Pentanedione on Cesium Doped Hydroxyapatite Catalysts with Balanced Acid-Base Sites

Authors: Xinli Li, Liangwei Sun, Weixin Zou, Ping Cao, Zhi Chen, Congming Tang, and Lin Dong

To be cited as: *ChemCatChem* 10.1002/cctc.201701332

Link to VoR: http://dx.doi.org/10.1002/cctc.201701332

A Journal of ChemPubSoc Europe

WILEY-VCH

www.chemcatchem.org

10.1002/cctc.201701332

Efficient Conversion of Bio-lactic Acid to 2,3-Pentanedione on Cesium Doped Hydroxyapatite Catalysts with Balanced Acid-Base Sites

Xinli Li[a], Liangwei Sun[b], Weixin Zou[c], Ping Cao[a], Zhi Chen[a], Congming Tang*[a,b], and Lin Dong[c]

Abstract: We report the design and synthesis of cesium doped hydroxyapatite for direct and high-yield conversion of bio-lactic acid to 2,3-pentanedione (72.3%). Cs species derived from $CsNO_3$ at high temperature of calcination is introduced into the hydroxyapatite structure to regulate its acid-base properties. It is found that a balance of acid-base chemistry favors the condensation of lactic acid to 2,3-pentanedione. As a result, the undesired reactions such as lactic acid dehydration, decarbonylation and coking are suppressed. Instead, a concerted catalysis between surface basic site and acidic site for lactic acid condensation to 2,3-pentanedione dominates on the cesium doped hydroxyapatite catalyst, leading to a highly selective process for direct conversion of bio-lactic acid to 2,3-pentanedione.

Introduction

Chemicals and fuels are obtained from abundant, renewable biomass and its derivatives via catalytic conversion, which provides a viable route to alleviate our strong dependence on increasingly depleting fossil fuels.[1] For that reason, lactic acid (LA) is particularly attractive due to its facile synthesis by biomass fermentation together with chemical conversion of glycerol, and expected increased availability and reduced cost.[2] Recent years, conversion of LA into chemicals such as acrylic acid,[3] acetaldehyde,[4] poly-lactic acid,[5] and 2,3-pentanedione[6] has become a heated topic for the chemical industry to decrease the use of petrochemical reserves. Currently, synthesis of 2,3-pentanedione is mainly via oxidation of methyl propyl ketone in the presence of hydroxylamine hydrochloride catalyzed by $NaNO_2$ and HCl.[7] Besides, it can also be obtained by condensation of acetol with hexanal catalyzed by acid. Here, a promising opportunity arises to replace petroleum-based feedstock by renewable lactic acid for greener and more sustainable 2,3-pentanedione production.

In the past decades, the investigation on condensation of LA into 2,3-pentanedione has focused on carbon/silicon supported on alkali metal nitrates or phosphates as catalysts.[6, 7b-d] Although the reaction conditions are optimized, these catalysts have displayed an unsatisfied performance, ca., low 2,3-pentanedione selectivity and high acrylic acid selectivity. For example, over the 9%$NaNO_3$/SBA-15 catalyst at 340°C, the selectivities of 2,3-pentanedione and acrylic acid are 62.1% and 18.4%, respectively, and LA conversion is low, only 58.8%.[6b] Furthermore, most of all these catalysts are short of evidence of catalyst stability. Thus these have prompted us to further investigate on the relation between the property derived from catalyst structure as well as its components and activity to achieve an efficient catalyst for condensation of LA into 2,3-pentanedione. Hydroxyapatite is used as biomedical materials due to an excellent biocompatibility. Recently, it is also extended to efficient catalysts for dehydration of LA to acrylic acid.[3d, 8] In comparison with its bare form, the modified hydroxyapatite displayed better properties in application.[9] For example, in zinc incorporated hydroxyapatite, the preference of Zn for the Ca2 site may facilitate uptake and release of Zn by biological hydroxyapatite.[10]

In this work, we developed a novel approach for preparation of cesium doped hydroxyapatites, and investigated their catalytic performance for condensation of LA to 2,3-pentanedione. In experiments performed to date, 2,3-pentanedione yields as high as 72.3% have been achieved, with acetaldehyde and acrylic acid, both being still valuable, as byproducts. More importantly, the catalyst is very stable for at least 40 h on stream (Figure 1). The unprecedented catalytic performance relates to synergy between basic sites and acidic sites located on the surface of cesium doped hydroxyapatite catalyst.

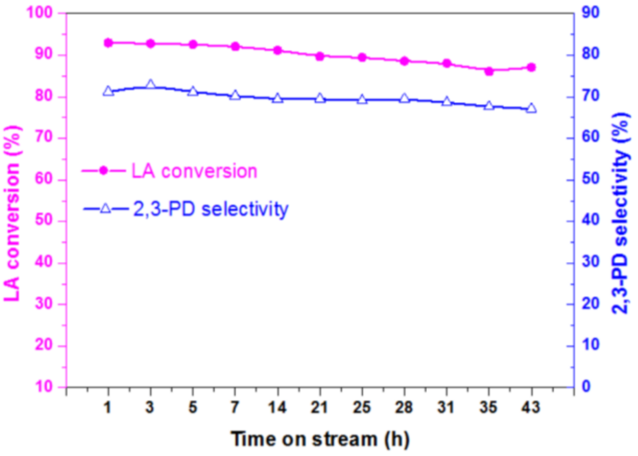

Figure 1. LA conversion and 2,3-pentanedione selectivity vs time on stream using cesium doped hydroxyapatite. (a: Catalyst, 0.38 mL, catalyst with Ca : P : Cs = 1.622 : 0.958 : 1.667, calcination temperature: 700°C, carrier gas N_2: 1 mL/min, feed flow rate: 1 mL/h, LA feedstock: 20wt% in water, reaction temperature, 290 °C. b: LA: lactic acid, 2,3-PD: 2,3-pentanedione.)

---

[a] Xinli Li, Ping Cao, Zhi Chen and Prof. Congming Tang
School of Chemistry and Chemical Engineering
Chongqing University of Technology
Chongqing 40054, PR China
E-mail: tcmtang2001@163.com (C. M. Tang)
[b] Liangwei Sun
Chemical Synthesis and Pollution Control Key Laboratory of Sichuan Province
China West Normal University
Nanchong, Sichuan, 637002, PR China
[c] Weixin Zou and Prof. Lin Dong
Jiangsu Key Laboratory of Vehicle Emissions Control, Center of Modern Analysis,
Nanjing University, Nanjing 210093, PR China

Supporting information for this article is given via a link at the end of the document.

10.1002/cctc.201701332

Results and Discussion

Catalyst characterization

To incorporate the multiple functionality needed for a catalytic conversion of process that directly converts bio-lactic acid to 2,3-pentanedione, a number of cesium doped hydroxyapatite materials were prepared by the means of inducing cesium component and high–temperature calcination, which favors cesium component dispersion in the structure of hydroxyapatite to regulate acid-base properties. The physical properties of these catalyst materials will be firstly described.

Hydroxyapatite and cesium doped hydroxyapatite materials with varying Ca/Cs ratios, unless otherwise noted, were prepared with one-pot synthesis, and characterized by XRD, FT-IR, SEM-EDX, surface area / pore size measurements. Figure 2 showed the wide-angle X-ray diffraction (XRD) patterns of catalyst materials with Ca : P : Cs = 1.622 : 0.958 : 1 at different calcination temperatures. Hydroxyapatite phase is confirmed among all the samples except for the sample calcined at 800ºC. $CsNO_3$ phase is also evidently determined in the samples which were calcined at lower 600 ºC, and it disappears with further increase of calcination temperatures, ca. 700ºC. Although $CsNO_3$ disappears at higher than 700ºC, Cs is doped homogeneously into the structure of hydroxyapatite, which is confirmed by EDX analysis (Figure S1, A) together with its corresponding elemental mapping (Figure S1, B). These similar phenomena were also observed in the samples with different Cs doped amounts at calcination temperature of 700ºC (Figure 3). However, the $CsNO_3$ phase occurred obviously when the Cs doped amount increased largely, ca., ratio of Ca : P : Cs being up to 1.622 : 0.958 : 2.333. Samples (a-g) can hardly observe the characteristic diffraction peaks for $CsNO_3$ phase since the calcination temperature (700ºC) is higher than its discomposed temperature (600ºC). Furthermore, the diffraction peaks indexed to hydroxyapatite also reduce in peak intensity, suggesting that Cs is well doped into structure of hydroxyapatite. To obtain further insight into Cs-hydroxyapatite support interactions, we studied the oxidation state of Cs in catalyst before and after calcination at 700 ºC by X-ray photoelectron spectroscopy (XPS, Figure 4). The binding energy (BE) was corrected for surface charging by taking the C 1s peak of contaminant carbon as a reference at 284.6 eV. The Cs $3d_{5/2}$ BE in the catalyst calcined at 700 ºC is about 723.36 eV, lower than that before calcination (723.76 eV). This phenomenon can be explained that before calcination at 700 ºC, Cs combines with NO_3^-, while Cs changes to combine with PO_4^{3-} after calcination because NO_3^- decomposes at high temperature. Electronegativity for N element is stronger than P element. This also confirmed that Cs component is well doped into the structure of hydroxyapatite. In addition, FT-IR spectra is also used to investigate the structure of catalyst (Figure S2 and 3). Absorption band at ~1396 cm^{-1} ascribed to NO_3^- disappears when the calcination temperature increases to 700ºC while the new absorption band at ~ 910 cm^{-1} occurs, which confirms the strong interaction between Cs and PO_4^{3-} (Figure S2). At higher Cs content, the absorption band at ~1385 cm^{-1} indexed to aggregation of a separate $CsNO_3$ phase could be observed (Figure S3), in agreement with the XRD results.

Nitrogen physisorption results show in Table S1 and 2. The specific surface area reduces from 38.3 to 2.0 m^2/g with increase of calcination temperature while the average pore size for all samples remains 3.8 nm (Table S1). From the results showed in Table S2, the specific surface area for samples with varying Cs contents slightly fluctuates between 7.2 and 9.1 m^2/g. Similarly, the average pore size also ranges from 3.4 to 3.8 nm.

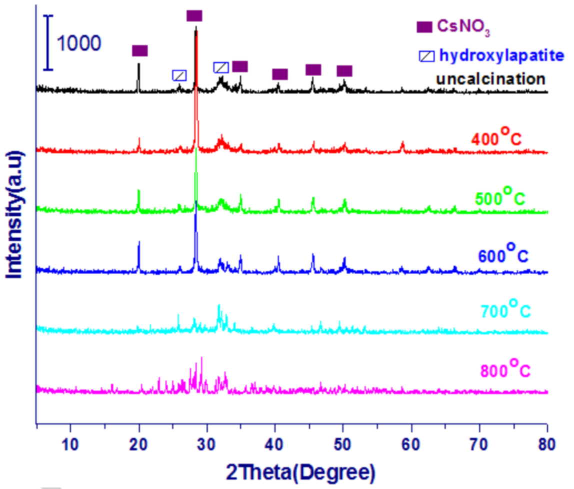

Figure 2. XRD patterns of catalysts at different calcination temperatures (Ca : P : Cs = 1.622 : 0.958 : 1)

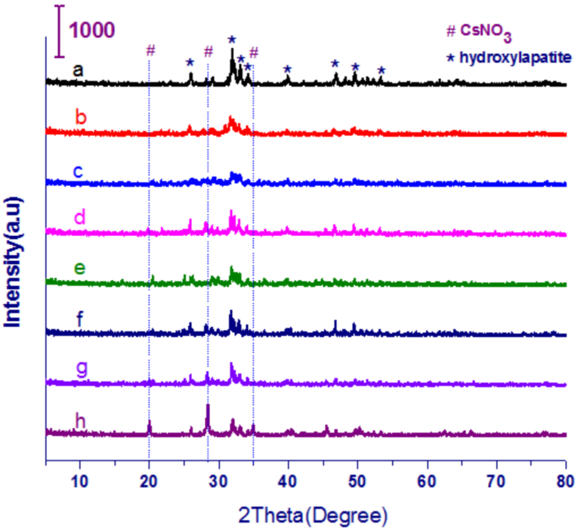

Figure 3. XRD of catalyst with different loading $CsNO_3$ amount at calcination temperature of 700ºC

a : Ca : P = 1.622 : 0.958, b : Ca : P : Cs = 1.622 : 0.958 : 0.334, c : Ca : P : Cs = 1.622 : 0.958 : 0.667, d : Ca : P : Cs = 1.622 : 0.958 : 1, e : Ca : P : Cs = 1.622 : 0.958 : 1.333, f : Ca : P : Cs = 1.622 : 0.958 : 1.667, g : Ca : P : Cs = 1.622 : 0.958 : 2, h : Ca : P : Cs = 1.622 : 0.958 : 2.333

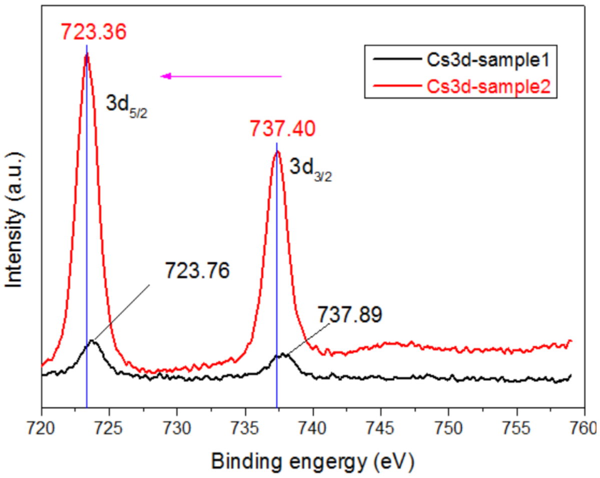

Figure 4. XPS spectra of catalyst (Ca : P : Cs=1.622 : 0.958 : 1) before and after calcination at 700°C (sample 1, uncalcination; sample 2, calcined at 700 °C)

Catalytic performance

Table 1 shows the performance of hydroxyapatite doped with Cs at different calcination temperatures for the condensation reaction of LA to 2,3-pentanedione. Initially, LA conversion lineally increases with an increase of calcination temperature, up to 700 °C, and then it decreases drastically with further increase of calcination temperature. In contrast with effect of calcination temperature on LA conversion, the selectivity to 2,3-pentanedione is relatively sensitive to calcination temperature. When the calcination temperature increases from 120°C (drying temperature) to 700 °C, the selectivity to 2,3-pentanedione increases from 42.1% to 66.9%. But more than 700 °C, the selectivity to 2,3-pentanedione also drastically decreases. For example, at calcination temperature of 900 °C, 2,3-pentanedione is hardly detected, and LA conversion is very low, only ~10%. Again, correlating the catalyst performance with its calcination temperature discloses that volcano-type dependence appears between 2,3-pentanedione production rate and calcination temperature, which reveals an important factor of choosing calcination temperature for selective production of 2,3-pentanedione, 700 °C being the optimal calcination temperature in our experiment conditions performed for condensation reaction of LA into 2,3-pentanedione. Under the fixed calcination temperature (700 °C), we further investigate the effect of Cs doped amount on the catalytic performance (shown in Table 2). On the bare hydroxyapatite catalyst (without Cs component), the catalytic activity is very low, LA conversion being around 10%, and 2,3-pentanedione is hardly detected. It is noted that hydroxyapatite is an excellent catalyst for dehydration of LA to acrylic acid, and low 2,3-pentanedione selectivity (around 1%) is reported at 360°C of reaction temperature.[3d, 8a] When a small amount of Cs component is doped into hydroxyapatite structure (Ca/Cs molar ratio = 1.622 : 0.334), LA conversion of 50.5% as well as 2,3-pentanedione selectivity of 54.3% is achieved, indicating that additional catalytic chemistry is taking place. In the range of low content of Cs (Ca/Cs molar ratio > 1.622 : 1), catalytic activity increases with an increase of Cs content. However, catalytic activity remains constant (~90% of LA conversion and 70% of 2,3-pentanedione selectivity) when Cs content is above 1 : 1.622 for Cs/Ca molar ratio. But excessive Cs content such as Cs/Ca molar ratio = 2.33 : 1.622 does not favor the catalytic performance (LA conversion = 70% and 2,3-pentanedione selectivity = 60.9%). To the best of our knowledge, direct conversion of LA to 2,3-pentanedione with both a high selectivity (~70%) and a high LA conversion (~90%) has never been reported. These observations indicate that calcination and the Cs-doped amount enable improvement of acid-base properties of the hydroxyapatite for direct conversion of LA to 2,3-pentanedione.

Table 1. Catalytic Activity Results for Hydroxyapatite Doped with Cs at Different Calcination Temperatures[a]

Calcined temp./°C	LA conv. [%]	Sel. [%][b]					Area-specific catalytic rate ($\mu mol\cdot h^{-1}\cdot m^{-2}$)	
		2,3-PD	AD	PA	AA	ACA	LA consumption	PD formation
-	72.5	42.1	16.0	7.7	15.4	6.2	103	22
400	73.6	53.7	11.7	7.2	17.7	6.1	325	88
500	76.9	59.8	9.5	7.2	17.8	1.5	428	128
600	88.2	64.6	10.9	6.4	15.6	1.7	564	182
700	89.9	66.9	10.1	6.2	15.1	1.4	831	278
800	51.4	65.5	7.4	8.0	14.0	1.8	744	243
900	~ 10	-					617	-

a: Catalyst, 0.38 mL, Ca/P/Cs = 1.622:0.958:1, particle size: 20~40 meshes, carrier gas N_2: 1 mL/min, feed flow rate: 1 mL/h, LA feedstock: 20wt% in water reaction temperature, 300°C, TOS: 4~5 h. b: LA: lactic acid, 2,3-PD: 2,3-pentanedione, AD: acetaldehyde, PA: propionic acid, AA: acrylic acid, ACA: acetic acid.

Table 2. Effect of Cs Doped Amount on Catalytic Performance of the Condensation Reaction of LA[a]

Ca/Cs molar ratio	LA conv. [%]	Sel. [%][b]					Area-specific catalytic rate ($\mu mol\cdot h^{-1}\cdot m^{-2}$)	
		2,3-PD	AD	PA	AA	ACA	LA consumption	PD formation
1.622 : -	~10	-					98	-
1.622 : 0.334	50.5	54.3	2.8	9.1	10.5	3.1	457	124
1.622 : 0.667	66.7	68.8	8.1	7.9	11.1	2.4	646	222
1.622 : 1	89.9	66.9	10.1	6.2	15.1	1.4	831	278
1.622 : 1.333	90.5	69.2	9.2	6.6	13.2	1.6	866	300
1.622 : 1.667	91.4	69.9	9.3	5.4	13.9	1.2	906	317
1.622 : 2	86.3	72.7	8.6	5.9	11.1	1.4	789	287
1.622 : 2.33	70	60.9	14.6	8.7	12.7	2.8	823	251

a: Catalyst, 0.38 mL, fixed Ca / P molar ratio = 1.622 : 0.958, calcination temperature: 700°C, particle size: 20~40 meshes, carrier gas N_2: 1 mL/min, feed flow rate: 1 mL/h, LA feedstock: 20wt% in water, reaction temperature, 300ºC, TOS: 4~5 h. b: LA: lactic acid, 2,3-PD: 2,3-pentanedione, AD: acetaldehyde, PA: propionic acid, AA: acrylic acid, ACA: acetic acid.

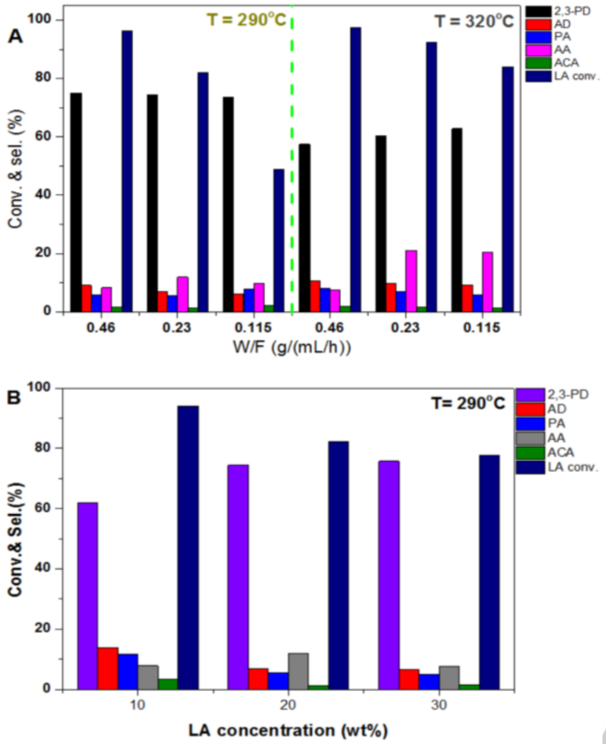

Figure 5. performance of catalyst with Ca : P : Cs = 1.622 : 0.958 : 1.667 for the condensation of LA as a function of residence time and reaction temperature (**A**), and effect of LA concentration at 290 ºC (**B**). a: 0.23g of catalyst, calcination temperature: 700ºC, LA concentration: 20 wt%, TOS: 4~5 h. b: LA: lactic acid, 2,3-PD: 2,3-pentanedione, AD: acetaldehyde, PA: propionic acid, AA: acrylic acid, ACA: acetic acid.

Multiple factors including reaction temperature, residence time, and LA concentration were found to affect LA conversion and 2,3-pentanedione selectivity on the hydroxyapatite doped with Cs (Ca : P : Cs = 1.622 : 0.958 : 1.667). LA conversion drastically increases while 2,3-pentanedione selectivity has only a slight fluctuation with residence time (Figure 5A), suggesting that condensation reaction of LA to 2,3-pentanedione dominates. In addition, we also found that with an increase of reaction temperature, the selectivity to 2,3-pentanedione decreases while the selectivities to by-products such as acetaldehyde and acrylic acid increase. Under a relatively low reaction temperature (290ºC), the effect of LA concentration on reaction performance was investigated (Figure 5B). 2,3-Pentanedione selectivity increases with an increase of LA concentration while LA conversion decreases. According to previous kinetic studies, formation of 2,3-pentanedione from LA via condensation reaction is second order in LA concentration while other accompanied conversion reactions of LA to acrylic acid and acetaldehyde is first order in LA concentration.[7c, 7d] Thus elevated LA concentration favors the formation of 2,3-pentanedione, to improve 2,3-pentanedione selectivity. Importantly, note that 2,3-pentanedione yields as high as 72.3% were obtained under the optimal reaction conditions tested in these studies (Figure 5A).

The reaction mechanism on condensation of LA to 2,3-pentanedione has been investigated over the sodium salts/silica or silica-alumina catalysts.[6b, 7a, 7d] In those studies, the sodium lactate in-situ formed via reaction of initial sodium salts with lactic acid is believed as an important stable intermediate for conversion of LA to 2,3-pentanedione, and is confirmed by experimental evidence. In the process for formation of 2,3-pentanedione from LA, the two key steps including decarboxylation of LA and ketonization accompanying with loss of water are involved. The catalyzed decarboxylation reaction requires basic sites while the catalyzed ketonization with loss of water requires acidic sites. In other words, developing a bifunctional catalyst which possesses both acidic sites and basic sites on its surface has a potential chance for catalyzing the condensation of LA to 2,3-pentanedione efficiently. According to previous studies, hydroxyapatite has been found to have an excellent activity for dehydration of LA due to the presence of the appropriate acidic sites on its surface.[3d, 8a, 11] For that reason, hydroxyapatite has been chosen as a catalyst support due to an existence of appropriate acidic sites for dehydration reaction of LA and its derivatives. But, possessing inherent acid-base properties on its surface can not well catalyze the condensation of LA to 2,3-pentanedione. Thus under the high temperature calcination, active precursor ($CsNO_3$) has been doped into its structure to regulate acid-base properties via in-situ synthesis by means of one-pot method, and the results has been shown in Figure 6, S4 and S5. Acidity density characterized with NH_3-TPD increases linearly when calcination temperature is enhanced, but a volcano-type appears between basicity density characterized with CO_2-TPD and calcination temperature. Due to this, basicity/acidity ratio functions as calcination temperature, obtaining a similar volcano-type curve. Furthermore, we correlated area-specific catalytic rates including LA consumption rate and 2,3-pentanedione formation rate with basicity/acidity ratio, and the results were shown in Figure 7. The area-specific catalytic rates increase slowly with basicity/acidity ratio in the range from 4.0 to 7.5, but decrease drastically as the basicity/acidity ratio is lower than 4.0. From the data shown in Figure 7, it seems that catalytic activity for conversion of LA to 2,3-pentanedione continuously increases with enhancement of basicity/acidity ratio under the ratio of basicity/acidity > 4. But this is not true from the data shown in Table 2 together with Figure 6B. For example, the basicity/acidity ratio is more than 19 on bare hydroxyapatite (without Cs doped amount), while the activity for condensation reaction of LA to 2,3-pentanedione is very low, LA conversion being ~10%. Interestingly, the Cs component is doped into the structure of hydroxyapatite, resulting in a rapid decrease of the basicity/acidity ratio, and it remains to 7~8 although the Cs doped amount changes. The results were supported by the evidence obtained with the diffuse reflectance infrared Fourier transform spectra (DRIFTS) of adsorbed pyridine on catalysts because Brönsted acidic sites and Lewis sites increased in contrast with bare hydroxyapatite (Figure S6). More importantly, all these catalysts with doped Cs offer an acceptable selectivity to 2,3-pentanedione (54.3~72.7%). From the above observations, we can conclude that both calcination temperature and Cs doped amount can provide a balance of surface acid-base chemistry in the Cs doped hydroxyapatite, which favors the activity for condensation of LA to 2,3-pentanedione.

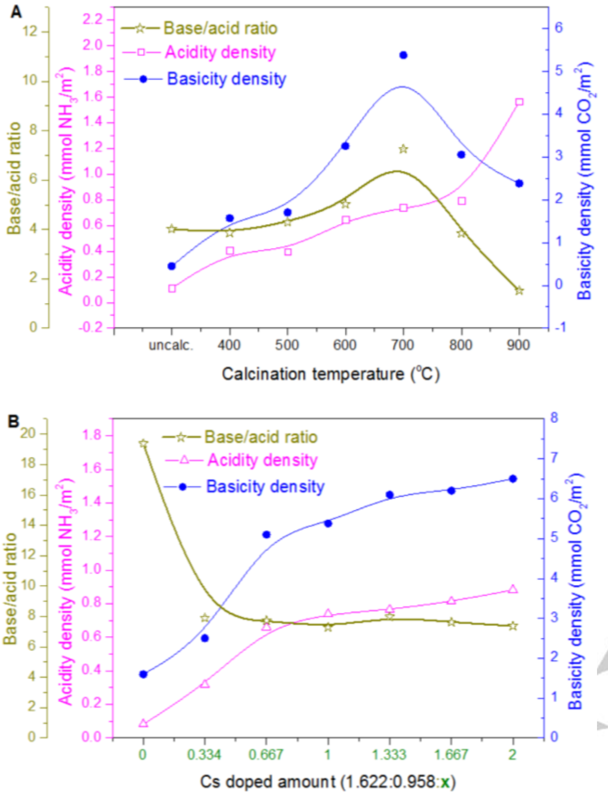

Figure 6. The acid-base properties of catalysts versus calcination temperature (**A**, (Ca : P : Cs=1.622 : 0.958 : 1)) and the Cs doped amount (**B**, calcination temperature, 700°C)

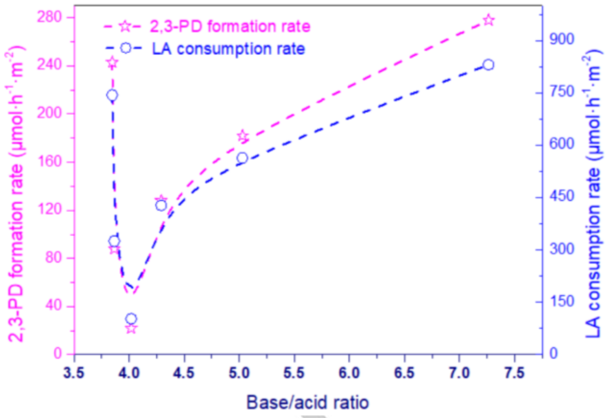

Figure 7. Catalytic rate versus base/acid ratio

Based on these experimental evidences, the possible reaction mechanism was proposed (shown in Scheme 1 and S1). In the mechanism, two steps are crucial for the formation of 2,3-pentanedione from lactic acid. Step 1, the basic sites on the surface of catalyst attack H at α-carbon to produce an enolate form (I). After deprotonation, the process undergoes a Claisen condensation, followed by decarboxylation to produce form (II). In this step, a large number of CO_2 was detected while only trace of CO was detected in the on-line reaction tail gas analysis (shown in Figure S7). Step 2, acidic sites attack β-OH of form (II) to remove a molecular water, and form another enolate (III). Form (III) rapidly isomerizes into product of 2,3-pentanedione.

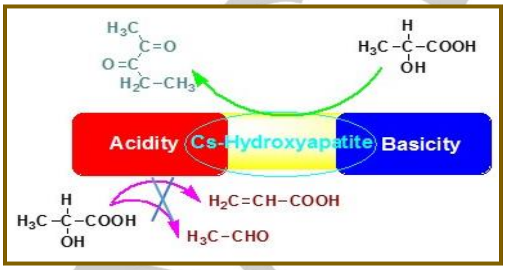

Scheme 1. Proposed mechanism for the condensation of LA to 2,3-pentanedione. Reaction process highlighted in green is preferred pathway, while the pink highlighted steps are undesirable ones. Detailed reaction pathways see **Scheme S1**.

Conclusions

We report efficient conversion of bio-lactic acid to 2,3-pentanedione, a highly value-added fine chemical useful for flavoring chemicals, using a multifunctional cesium doped hydroxyapatite catalyst. The unique modification of cesium doped hydroxyapatite provides a balance of the surface acid-base chemistry in the catalyst. Consequently, undesirable reactions such as dehydration and decarbonylation of lactic acid which are mainly believed to catalyze by acidic sites, are largely suppressed, while the surface basic site-acidic site synergically catalyzed lactic acid condensation reaction to 2,3-pentanedione dominates on the cesium doped hydroxyapatite. In this way, a highly selective (as high as 72.3% yield) process for direct conversion of bio-lactic acid to 2,3-pentanedione on the cesium doped hydroxyapatite has been achieved.

Experimental Section

Materials

Lactic acid (85~90 wt%) was purchased from Chengdu Kelong Chemical Reagent Co. and was used for the synthesis of 2,3-pentanedione without further purification. Triple-distilled water was prepared in the laboratory and was used to dilute lactic acid for demanded concentration. Cesium nitrate, $Ca(OH)_2$, H_3PO_4, 2,3-pentanedione, propionic acid, acetaldehyde, acrylic acid, acetic acid and n-butanol, together with hydroquinone were purchased from Sinopharm Chemical Reagent Co., Ltd. 2,3-Pentanedione, propionic acid, acetaldehyde, acrylic acid and acetic acid were used for gas chromatograph reference materials, and n-butanol was utilized as internal standard material. Hydroquinone (0.3 wt %) was used as a polymerization inhibitor.

Preparation of catalysts

The Cs doped hydroxyapatite catalysts were prepared by an evaporation-driven oriented assembly (EDOA) approach in a basic $Ca(OH)_2/H_3PO_4/H_2O/CsNO_3$ mixed solution. Typically, for Cs doped hydroxyapatite with Ca : P : Cs = 1.622 : 0.958 : 1, 1.85 g (25 mmol) of $Ca(OH)_2$ was dissolved in 100 mL H_2O, and stirred vigorously for 30 min to form a clear and transparent solution. Sequentially, 1.0 mL (14.76mmol) of H_3PO_4 (85 wt%) was added dropwise under vigorous stirring for 60 min to form a white murky solution. Next, 3.0 g (15.41mmol) of $CsNO_3$ was added to the resultant solution under vigorous stirring for 300 min. After that, the obtained solution was transferred into a volumetric flask, and left it in a drying oven to evaporate solvent H_2O at 70 ºC for 8 h, then second-step evaporate at 100 ºC for another 10 h to completely remove the solvent. The obtained white powder was calcined at 700 ºC for 600 min to use as a catalyst for LA condensation to 2,3-pentanedione. The bare hydroxyapatite (without Cs component) was prepared using a similar method.

Catalyst characterization

Powder X-ray diffraction measurement was conducted on a Dmax/Ultima IV diffractometer operated at 40 kV and 20 mA with Cu-Ka radiation. The FTIR spectra of the catalysts were recorded in the range of 500~4000 cm^{-1} on a Nicolet 6700 spectrometer. The morphologic features of the catalysts were determined by scanning electron microscope (SEM, JSM-6510). The specific surface areas of catalysts were measured through nitrogen adsorption at 77 K using Autosorb IQ instrument. Prior to adsorption, the samples were treated at 250 ºC under vacuum for 6 h and the specific surface area was calculated according to the Brunauer-Emmett-Teller (BET) method. Surface acid and base properties of the samples are estimated by NH_3-TPD and CO_2-TPD, respectively, on a Quantachrome Instrument. The sample (ca. 50~60 mg) is purged with dry Ar (50 mL/min, purity> 99.999*vt*%) at 400ºC for 1.0 h, followed by reducing the furnace temperature to room temperature, and switching to a flow of 8v_t% NH_3/Ar or 10 v_t% CO_2/Ar for 1 h to execute NH_3 or CO_2 adsorption. Then, NH_3 or CO_2 adsorbed on the sample is desorbed in the range of 80~600ºC at a rate of 10 ºC/min. FTIR of adsorbed pyridine experiments were performed on a Bruker Tensor 27 FTIR spectrometer equipped with Praying Mantis™ accessory and a high-pressure reaction cell (Harrick Scientific Products Inc.) for *in situ* Diffuse Reflectance Infrared Fourier Transform spectroscopy (DRIFTS) measurements. Briefly, ~50 mg of finely ground sample was loaded in the reaction cell. The sample was then ramped to 400 ºC (10 ºC/min) for *in-situ* purging under flowing pure Ar (flow rate 15 mL (STP)/min). After holding at 400 ºC for 2 hours, the sample was cooled to ambient temperature in pure Ar (15 mL (STP)/min), a background spectrum was then taken. Pyridine was introduced into the reaction cell by flowing He (5 mL (STP)/min) through a bubble generator at ambient temperature until saturation (judged by the appearance of the 1596 cm^{-1} feature assigned to physisorbed pyridine). Physisorbed pyridine was removed with pure Ar purging (15 mL (STP)/min) at 100ºC. The sample was then cooled to ambient temperature and IR spectra were acquired. X-ray photoelectron spectroscopy (XPS) measurements were performed using a Thermo Scientific K-Alpha spectrometer, equipped with a monochromatic small-spot X-ray source and a 180º double focusing hemispherical analyzer with a 128-channel detector. Spectra were obtained using an aluminum anode (Al Kα = 1486.6 eV) operating at 72 W and a spot size of 400 μm. Survey scans were measured at a constant pass energy of 200 eV and region scans at 50 eV. The background pressure was 2×10^{-9} mbar and during measurement 3×10^{-7} mbar Argon because of the charge compensation dual beam source. Data analysis was performed using CasaXPS software. The binding energy was corrected for surface charging by taking the C 1s peak of contaminant carbon as a reference at 284.6 eV.

Catalyst evaluation

The condensation of lactic acid to 2,3-pentanedione over the catalysts was carried out in a fixed-bed quartz tubular reactor with a 4 mm inner diameter operated at atmospheric pressure. The catalyst (ca. 0.23~0.25 g, 20~40 meshes) was placed in the middle of the reactor and quartz wool was placed in both ends. Firstly, the catalyst was pretreated at the required reaction temperature (ca. 300 °C) for 1.5 h under N_2 with high purity (0.1 MPa, 1.0 mL/min). The feedstock (20 wt% solution of LA) was then pumped into the reactor (LA aqueous solution flow rate, 1.0 mL/h) and driven through the catalyst bed by nitrogen. Residence time is calculated according to equation 1. The liquid products were condensed using ice-water bath and analyzed off-line using a SP-6890 gas chromatograph with a FFAP capillary column connected to a FID. Quantitative analysis of the products was carried out by the internal standard method using *n*-butanol as the internal standard material. GC-MS analyses of the samples were performed using Agilent 5973N Mass Selective Detector attachment. The reaction tail gas was analyzed using GC with a packed column of TDX-01 connected to TCD detector. The conversion of LA and the selectivity toward 2,3-pentanedione or other by-products were calculated according to equations 2, 3 and 4.

$$t_R = \frac{w}{F} \text{------ (1)}$$

t_R: Residence time ($h \cdot g \cdot mL^{-1}$); *w*.: catalyst mass (g); *F*: feed (LA aqueous solution) flow rate (mL/h).

$$Conversion / \% = \frac{n_0 - n_1}{n_0} \times 100 \text{----- (2),}$$

$$Selectivity / \% = \frac{n_p}{n_0 - n_1} \times 100 \text{------ (3),} \quad Yield / \% = \frac{n_p}{n_0} \times 100 \text{----- (4}$$

Where n_0 is the molar quantity of LA fed into reactor, n_1 is the molar quantity of LA in the effluent, and n_p is the molar quantity of lactic acid converted to 2,3-pentanedione or other byproducts such as acetaldehyde, propionic acid, acrylic acid, and acetic acid.

Acknowledgements

This work was supported by Sichuan province science and technology department application foundation project (2017JY0188）, the opening foundation of Jiangsu Key Laboratory of Vehicle Emissions Control (NO. OVEC 032), and Scientific Research Fund of Sichuan Provincial Educational Department (16ZA0175).

Keywords: cesium doped hydroxyapatite • 2,3-pentanedione • condensation • lactic acid • green synthesis

[1] a) P. Liu, E. J. M. Hensen, *J. Am. Chem. Soc.* **2013**, *135*, 14032-14035; b) J. M. Sun, K. K. Zhu, F. Gao, C. M. Wang, J. Liu, C. H. F.

Peden, Y. Wang, *J. Am. Chem. Soc.* **2011**, *133*, 11096-11099; c) L. S. Sharninghausen, J. Campos, M. G. Manas, R. H. Crabtree, *Nat. Commun.* **2014**, *5*, 1-7; d) D. M. Alonso, J. Q. Bond, J. A. Dumesic, *Green Chem.* **2010**, *12*, 1493-1513.

[2] a) M. Dusselier, P. Van Wouwe, A. Dewaele, E. Makshina, B. F. Sels, *Energy Environ. Sci.* **2013**, *6*, 1415-1442; b) J. L. Xu, H. Y. Zhang, Y. F. Zhao, B. Yu, S. Chen, Y. B. Li, L. D. Hao, Z. M. Liu, *Green Chem.* **2013**, *15*, 1520-1525; c) N. Murakami, M. Oba, M. Iwamoto, Y. Tashiro, T. Noguchi, K. Bonkohara, M. A. Abdel-Rahman, T. Zendo, M. Shimoda, K. Sakai, K. Sonomoto, *J. Biosci. Bioeng.* **2016**, *121*, 89-95; d) Y. L. Zhang, Z. Shen, X. F. Zhou, M. Zhang, F. M. Jin, *Green Chem.* **2012**, *14*, 3285-3288; e) Y. Li, M. Nielsen, B. Li, P. H. Dixneuf, H. Junge, M. Beller, *Green Chem.* **2015**, *17*, 193-198.

[3] a) X. H. Zhang, L. Lin, T. Zhang, H. O. Liu, X. F. Zhang, *Chem. Eng. J.* **2016**, *284*, 934-941; b) G. M. Lari, B. Puertolas, M. S. Frei, C. Mondelli, J. Perez-Ramirez, *ChemCatChem* **2016**, *8*, 1507-1514; c) Z. Guo, D. S. Theng, K. Y. Tang, L. L. Zhang, L. Huang, A. Borgna, C. Wang, *Phys. Chem. Chem. Phys.* **2016**, *18*, 23746-23754; d) B. Yan, L. Z. Tao, Y. Liang, B. Q. Xu, *ACS Catal.* **2014**, *4*, 1931-1943; e) J. S. Peng, X. L. Li, C. M. Tang, W. Bai, *Green Chem.* **2014**, *16*, 108-111.

[4] a) C. M. Tang, Z. J. Zhai, X. L. Li, L. W. Sun, W. Bai, *J. Catal.* **2015**, *329*, 206-217; b) B. Katryniok, S. Paul, F. Dumeignil, *Green Chem.* **2010**, *12*, 1910-1913.

[5] A. J. Amass, K. L. R. N'Goala, B. J. Tighe, F. Schue, *Polymer* **1999**, *40*, 5073-5078.

[6] a) L. W. Sun, X. L. Li, C. M. Tang, *Acta Phys. -Chim. Sin.* **2016**, *32*, 2327-2336; b) J. F. Zhang, X. Z. Feng, Y. L. Zhao, W. J. Ji, C. T. Au, *J. Ind. Eng. Chem.* **2014**, *20*, 1353-1358.

[7] a) M. S. Tam, G. C. Gunter, R. Craciun, D. J. Miller, J. E. Jackson, *Ind. Eng. Chem. Res.* **1997**, *36*, 3505-3512; b) D. C. Wadley, M. S. Tam, P. B. Kokitkar, J. E. Jackson, D. J. Miller, *J. Catal.* **1997**, *165*, 162-171; c) G. C. Gunter, R. H. Langford, J. E. Jackson, D. J. Miller, *Ind. Eng. Chem. Res.* **1995**, *34*, 974-980; d) G. C. Gunter, D. J. Miller, J. E. Jackson, *J. Catal.* **1994**, *148*, 252-260; e) M. S. Tam, R. Craciun, D. J. Miller, J. E. Jackson, *Ind. Eng. Chem. Res.* **1998**, *37*, 2360-2366.

[8] a) V. C. Ghantani, S. T. Lomate, M. K. Dongare, S. B. Umbarkar, *Green Chem.* **2013**, *15*, 1211-1217; b) A. Fihri, C. Len, R. S. Varma, A. Solhy, *Coordination Chemistry Reviews* **2017**, *347*, 48-76.

[9] K. Kaneda, T. Mizugaki, *ACS Catal.* **2017**, *7*, 920-935.

[10] Y. Z. Tang, H. F. Chappell, M. T. Dove, R. J. Reeder, Y. J. Lee, *Biomaterials* **2009**, *30*, 2864-2872.

[11] Y. Matsuura, A. Onda, S. Ogo, K. Yanagisawa, *Catal. Today* **2014**, *226*, 192-197.

Entry for the Table of Contents (Please choose one layout)

Layout 1:

FULL PAPER

1. Cesium doped hydroxyapatite catalysts offered an efficient activity for condensation of lactic acid to 2,3-pentanedione.

2. The unprecedented catalytic performance relates to synergy between basic sites and acidic sites located on the surface of cesium doped hydroxyapatite catalyst.

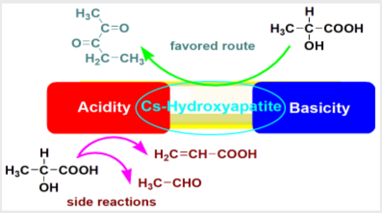

Xinli Li, Liangwei Sun, Weixin Zou, Ping Cao, Zhi Chen, Congming Tang, and Lin Dong*

Page No. – Page No.

Efficient Conversion of Bio-lactic Acid to 2,3-Pentanedione on Cesium Doped Hydroxyapatite Catalysts with Balanced Acid-Base Sites